Efficient malicious information detection method based on set partitioning for large-scale Internet of Things

Yuhan Suo[a], Runqi Chai[a,*], Kaiyuan Chen[b,c,*], Senchun Chai[a], Wannian Liang[b] and Yuanqing Xia[a]

[a] *School of Automation, Beijing Institute of Technology, Beijing, 100081, China*

[b] *Vanke School of Public Health, Institute for Healthy China, Tsinghua University, Beijing, 100084, China*

[c] *The State Key Laboratory of Management and Control for Complex Systems, Institute of Automation, Chinese Academy of Sciences, Beijing, 100190, China*

arXiv:2502.11538v2 [cs.DC] 29 Jun 2025

ARTICLE INFO

Keywords:
IoT security
large-scale enterprise network
attack detection scheduling
set partitioning strategy
security analysis

ABSTRACT

With the large-scale integration of Internet of Things (IoT) into enterprise information management systems, organizations are pursuing digital transformation that hinges on real-time data insights—and yet face escalating security and governance risks. Detecting and responding to threats at scale without impairing system efficiency has therefore become a critical information-management and decision-support challenge for today's executives. This paper develops a distributed, gain-based anomaly-detection framework tailored to IoT-enabled enterprise systems, underpinned by an optimized sensor-subset partitioning strategy. Starting from the perspective of set partitioning strategies, this study analyzes the key factor that contributes to the performance differences between distributed and centralized algorithms. By examining the gain mutual influence of sensor subsets, an optimal set partitioning strategy is designed to minimize inter-subset mutual influence while enhancing intra-subset correlation. To further reduce the computational cost of gain updates, a suboptimal partitioning strategy based on Grassmann distance is proposed, improving the efficiency of selecting suspicious sensors. Theoretical analysis demonstrates that this approach effectively reduces the computational cost of gain updates while maintaining detection performance. Finally, simulation results validate the effectiveness of the proposed method in enhancing attack detection performance.

1. Introduction

With the rapid development of information technology, automation and intelligent systems are profoundly reshaping the way modern society operates. As a key supporting technology for this change, sensor networks have been widely used in various fields, including smart cities, the Internet of Things, and industrial manufacturing (Heo, Hong and Cho, 2009; Habibzadeh, Qin, Soyata and Kantarci, 2017; Hatami, Leinonen, Chen, Pappas and Codreanu, 2022; Wang, Wang, Su and Ge, 2020). By enabling comprehensive environmental monitoring, real-time data acquisition, and autonomous control, these networks significantly enhance the intelligence and decision-making capabilities of enterprise information management systems (Wei, Zhu, Zhang, Wang, Zou, Meng, Wu and Feng, 2022; Tao, Zhang, Cheng, Ren, Wang, Qi and Li, 2022; Ju, Wei and Li, 2023).

However, the proliferation of sensor deployments introduces complex security and governance challenges, as organizational decision makers must balance efficient system operation with the timely detection and response to emerging threats(Xie, Yan, Yao and Atiquzzaman, 2018). Especially in open and dynamic network environments, adversaries may interfere with the system's state estimation by means of data tampering and information deception, resulting in system malfunctions or even serious security incidents, bringing significant risks to infrastructure and key businesses (Ge, Han, Zhong and Zhang, 2019; Pang, Fan, Dong, Han and Liu, 2021; Smith, Dhillon and Carter, 2021). Therefore, in the context of large-scale distributed sensor networks, the development of an efficient and accurate security defense mechanism has emerged as a crucial research direction to ensure system stability and reliability.

Attack detection has long been a core area of research in cybersecurity, encompassing critical domains such as intrusion detection, anomaly detection, and fault diagnosis (Wang, Lu, Ma and Jin, 2025; Suo, Chai, Chai, Farhan,

*Corresponding author

yuhan.suo@bit.edu.cn (Y. Suo); r.chai@bit.edu.cn (R. Chai); kaiyuanchen@mail.tsinghua.edu.cn (K. Chen); chaisc97@bit.edu.cn (S. Chai); liangwn@ tsinghua.edu.cn (W. Liang); xia_yuanqing@bit.edu.cn (Y. Xia)

ORCID(s): 0000-0003-4083-8863 (R. Chai)

Zhao and Xia, 2024a; Li, Chen, Liu, Wang, Zhang and Yu, 2023; Li, Chen, Chen, Li, Wang, Lv and Sun, 2024; Zhang, Pan, Han, Chen, Wen and Xiang, 2021; Zhao, Xu, Li, Zhao, Wang and Wen, 2023; Balta, Pease, Moyne, Barton and Tilbury, 2023). Existing methods primarily fall into two categories: rule-based and learning-based approaches. Rule-based approaches rely on predefined security policies and pattern matching techniques, such as anomaly threshold settings and signature detection. For example, Wang et al. (2025) extracted topological relationships measured by individual nodes and used reconstruction residuals to pinpoint the location of injection attacks. Suo et al. (2024a) explored the Grassmann distance of opinion evolution direction and leveraged its latent characteristics to iteratively filter out malicious agents. Li et al. (2023) constructed a dynamic relationship between raw data and decrypted results to enable rapid detection of malicious attacks. In the realm of manufacturing system security, Li et al. (2024) developed detection rules based on processing procedures and key parameters, identifying network attacks through rule matching. However, rule-based approaches struggle to adapt to novel and complex attacks. In contrast, learning-based approaches leverage data-driven techniques such as statistical analysis, machine learning, and deep learning to detect and recognize attack patterns, offering superior generalization and adaptability (Zhang et al., 2021). For instance, Zhao et al. (2023) designed a data-driven attack detector based on subspace identification, detecting attacks by computing the system's stable kernel representation. Balta et al. (2023) proposed a detection framework based on digital twins, identifying attacks by analyzing controlled transient behaviors. To address traffic anomaly detection, Zhang, Xie, Xiao, Bai, Liu and Dong (2022) designed a model consisting of two adversarial sub-networks to learn the data distribution of normal traffic. And based on this, an anomaly detection method based on high anomaly suppression is proposed. Nevertheless, existing research indicates that these methods still face significant challenges in model training and data dependency (Li et al., 2024; Zhang et al., 2021). Thus, improving adaptability and computational efficiency while ensuring detection accuracy remains a critical research direction in attack detection.

Beyond the research of attack detection, enhancing the system's resilience is also crucial for ensuring stability. Secure state estimation aims to accurately recover the state of system even in the presence of attack. This problem has become a key research focus in the field of cyber-physical system security, particularly in control systems and distributed sensor networks (Ding, Han, Ge and Wang, 2020; Mustafa, Mazouchi and Modares, 2022). In distributed sensor networks, redundant information is considered essential for ensuring secure state estimation. Even when some sensors are compromised, redundancy allows the system to maintain normal operation (Shoukry, Nuzzo, Puggelli, Sangiovanni-Vincentelli, Seshia and Tabuada, 2017). However, identifying compromised sensors efficiently while avoiding the combinatorial explosion associated with NP-hard problems remains a major research challenge (Lu and Yang, 2023b; An and Yang, 2022; Lu and Yang, 2023a). To enhance system resilience, researchers have proposed various secure state estimation strategies. For instance, when core sensors are compromised, Xin, He and Long (2025) introduced an estimation method based on virtual sensors, integrating deep reinforcement learning for online optimization to improve estimation accuracy and reliability. This approach aligns well with the concept of redundant information. Xia and Zhou (2025) proposed a robust distributed Kalman filtering algorithm, which leverages attack detection and robust data fusion strategies to mitigate the impact of malicious network attacks, thereby enhancing the accuracy and stability of distributed state estimation. However, in large-scale distributed sensor networks, computational complexity remains a significant challenge. Balancing security and computational efficiency continues to be a pressing issue that requires further investigation in this field.

For large-scale networks, a sufficient condition to ensure system security is that each sensor can directly exclude potential attacked sensors from the neighbor set. For instance, the ADS algorithm proposed in literature Suo, Chai, Chai, Pang, Xia and Liu (2024c) aims to achieve this objective. However, the algorithm is centralized for each node, which means that its efficiency may decrease as the neighborhood cardinality increases. Given that a distributed approach can enhance the efficiency of a centralized algorithm, this paper explores the feasibility of extending the ADS algorithm into a distributed form. Existing studies indicate that distributed algorithms generally lag behind centralized ones in performance, with partitioning strategies considered one of the key factors influencing this gap (Mirzasoleiman, Karbasi, Sarkar and Krause, 2016).

Existing studies have shown that partitioning large-scale sets into subsets based on feature characteristics is an effective way to address the curse of dimensionality (Wang, Chen, Yang, Wan, Li and Luo, 2023). The key challenge lies in identifying and selecting informative features. To more effectively design partitioning strategies, this paper will extract the inherent characteristics of each sensor. Based on this, the paper aims to optimize the design of partitioning strategies to balance the combined effect of inter-subset benefits and intra-subset correlations. Through optimized partitioning strategy design, the goal of this paper is to narrow the performance gap between distributed and centralized ADS algorithms, achieving a trade-off between efficiency and performance in the suspicious sensor selection task.

The main contributions of this paper are summarized as follows: The concept of mutual influence is introduced to quantify the marginal benefit interference between different sensor subsets. Based on the observable space characteristics of sensors, this metric effectively guides the set partitioning process, aiming to minimize inter-subset mutual influence. To address the imbalance in sensor gain updates caused by differences in observable spaces within subsets, a suboptimal set partitioning strategy based on Grassmann distance is proposed. This strategy maximizes the correlation among elements within each subset while minimizing mutual influence between subsets, providing strong support for extending the ADS algorithm to its distributed form (D-ADS). Under the proposed set partitioning strategy, gain updates are required only within the selected subset, significantly reducing computational costs. Theoretical results demonstrate that the error in the probability distribution vector remains bounded, ensuring the detection performance of suspicious sensor selection while improving algorithm efficiency. Finally, extensive simulation results under various scenarios validate the effectiveness of the proposed algorithm.

This paper is organized as follows: Section II presents the system model and problem formulation, including the description of the sensor network, attacker model, and the suspicious sensor selection problem in dynamic environments. Section III focuses on the analysis of the key factors affecting the performance of distributed algorithms, particularly the mutual influence of benefits between subsets and the design of the set partitioning strategy based on Grassmann distance. Section IV evaluates the performance of the proposed strategies through numerical simulations. Finally, Section V concludes the paper by summarizing the main contributions, and suggesting potential directions for future research.

2. Problem Formulation

2.1. System Model

IoT systems usually observe production data and system operation status, which usually changes continuously. Therefore, as a theoretical type of article, the following mathematical model is used to describe this process. Consider a distributed sensor network that monitors the discrete-time linear time-invariant system state $x(k)$, as described in equation (1)

$$x(k+1) = Ax(k) + \omega(k), \tag{1}$$

where $x(k) \in \mathbb{R}^n$ and $\omega(k) \in \mathbb{R}^n$ represent the system state and process noise, respectively. Moreover, $\omega(k)$ follows a Gaussian distribution with zero mean and a positive definite covariance matrix Q, i.e., $\omega(k) \sim \mathcal{N}(0, Q)$.

The network is represented by an undirected graph $\mathcal{G} = (\mathcal{N}, \mathcal{E})$, where $\mathcal{N}$ and $\mathcal{E} \subseteq \mathcal{N} \times \mathcal{N}$ denote the set of sensors and the set of edges, respectively. The neighbor set of sensor i is denoted as $\mathcal{N}_i = \{j \in \mathcal{N} : (i,j) \in \mathcal{E}\}$. Thus, we obtain $\mathcal{N} = \mathcal{N}_1 \cup \mathcal{N}_2 \cup \ldots \cup \mathcal{N}_{|\mathcal{N}|}$. For sensor i, where $i \in \mathcal{N}$, its measurement model follows equation (2)

$$y_i(k) = C_i x(k) + v_i(k), \tag{2}$$

where $y_i(k) \in \mathbb{R}^m$ and $v_i(k) \in \mathbb{R}^m$ represent the measurement and measurement noise of sensor i, respectively. The matrix $A \in \mathbb{R}^{n\times n}$ in equation (1) and the matrix $C_i \in \mathbb{R}^{m\times n}$ in equation (2) are both real matrices with appropriate dimensions. Similarly, $v_i(k)$ follows a Gaussian distribution with zero mean and a positive definite covariance matrix R_i, i.e., $v_i(k) \sim \mathcal{N}\left(0, R_i\right)$. In this section, both the process noise $||\omega(k)||$ and the measurement noise $||v_i(k)||$ are upper-bounded by certain positive scalars.

Furthermore, for the neighbor set $\mathcal{N}_i$ of sensor i, the system $(A, [C_1^{\mathrm{T}}, ..., C_{|\mathcal{N}_i|}^{\mathrm{T}}]^{\mathrm{T}})$ is observable. The distributed estimator of sensor i is then given by equation (3)

$$\hat{x}_i(k+1) \quad = \quad A\hat{x}_i(k) + K_i(k)\left(y_i(k) - C_i\hat{x}_i(k)\right) - \lambda A \sum_{j\in\mathcal{N}_i}\left(\hat{x}_i(k) - \hat{x}_j(k)\right), \tag{3}$$

where $\hat{x}_i(k)$ is the estimate of the state $x(k)$ for sensor i, where $\hat{x}_i(0) = x(0)$. Additionally, $\hat{x}_j(k)$ represents the estimate of sensor j, $K_i(k)$ is the gain matrix, and λ is the consensus parameter, which takes values within the range $(0, \min(1/|\mathcal{N}_i|))$.

2.2. Attacker Model

To describe the attacker model in IoT, this paper considers a dynamic attack strategy (Suo et al., 2024c), At each moment k, the attacker selects communication links to launch FDIAs based on the dynamic attack strategy defined in Definition 1.

Definition 1. ***(Dynamic Attack Strategy)*** *For the sets of compromised sensors at two consecutive moments, $\mathcal{A}_k$ and $\mathcal{A}_{k-1}$, if they differ, i.e., $\mathcal{A}_k \neq \mathcal{A}_{k-1}$, we refer to this as a dynamic attack strategy. The difference between the two sets can be calculated as*

$$\Delta_k = (\mathcal{A}_k \backslash \mathcal{A}_{k-1}) \cup (\mathcal{A}_{k-1} \backslash \mathcal{A}_k). \tag{4}$$

Thus, over the entire time period T, the total number of changes in compromised sensors is given by $\Delta_T = \sum_{k=1}^{T-1} \Delta_k$.

At moment k, suppose that the estimated state $\hat{x}_j(k)$ of sensor j is compromised by injecting malicious data $z_{ij}(k)$ during its transmission to sensor i. The compromised estimation received by sensor i, denoted as $\hat{x}^a_{ij}(k)$, is given by

$$\hat{x}^a_{ij}(k) = \hat{x}_j(k) + z_{ij}(k). \tag{5}$$

In addition, the attacker's strategy satisfies the following Assumption 1.

Assumption 1. *For the attacker's strategy, the following assumptions are made:*

- *At any moment k, the number of compromised sensors q_i in the neighborhood of sensor i does not exceed half the size of the neighborhood, i.e., $q_i \leq \lfloor |\mathcal{N}_i|/2 \rfloor$ Yang and Lv (2021); Lu and Yang (2023a)*
- *At any moment k, if the attacker reselects the set of compromised sensors, the selection process is entirely random, and the attack intensity is balanced.*

2.3. Suspicious Sensor Selection Problem

Lemma 1 in literature Suo et al. (2024c) states that selecting the suspicious sensor set from the set $\mathcal{N}_i$ is an NP-hard problem and that the objective function can be transformed into a submodular function as shown in equation (6)

$$f_k\left(\mathcal{A}_{i,k}\right) = \left\| \Lambda_{i,k} \cdot [\mu_{ij}(k)]_{j \in \mathcal{N}_i} \right\|, \tag{6}$$

where $\Lambda_{i,k}$ is the augmented error matrix, which is obtained by summarizing the estimated error $||\hat{x}_i(k) - \hat{x}^a_{ij}(k)||$, i.e., $\Lambda_{i,k} = \sum_{j=1}^{|\mathcal{N}_i|} \left(\theta^j_{|\mathcal{N}_i|} \otimes ||\hat{x}_i(k) - \hat{x}^a_{ij}(k)|| \right)$, and $[\mu_{ij}(k)]_{j \in \mathcal{N}_i}$ denotes the augmented matrix of $\mu_{ij}(k)$, where $\mu_{ij}(k) = 1$ for $j \in \mathcal{A}_{i,k}$ and $\mu_{ij}(k) = 0$ for $j \in \mathcal{N}_i \backslash \mathcal{A}_{i,k}$. Consequently, the suspicious sensor selection problem is reformulated as a solvable submodular maximization problem under a cardinality constraint, as presented in Problem 1.

Problem 1. *Suo et al. (2024c) The problem of selecting suspicious sensors essentially involves choosing no more than q_i sensors to maximize the objective function (6), i.e.,*

$$\max_{\mathcal{A}_{i,k} \subseteq \mathcal{N}_i} f_k\left(\mathcal{A}_{i,k}\right), \quad s.t. \left|\mathcal{A}_{i,k}\right| \leq q_i, \tag{7}$$

where q_i is defined in Assumption 1.

3. Main Results

It is shown that distributed algorithms have obvious advantages over centralized algorithms in terms of efficiency, but from the perspective of performance, distributed algorithms generally have a certain gap with centralized algorithms. Therefore, this section focuses on the following issues: analyzing the key factors that affect the performance difference between D-ADS and ADS algorithm, and designing effective partitioning strategies to minimize the performance gap.

3.1. The mutual influence of benefits between subsets

In this section, the neighbor set of each sensor is divided into several subsets, and the ADS algorithm in the literature Suo et al. (2024c) is deployed on each subset. At this time, the ADS algorithm becomes a distributed case, that is, the D-ADS algorithm.

Specifically, the neighbor set $\mathcal{N}_i$ of sensor i is divided into m_i subsets, expressed as $\mathcal{N}_i = \mathcal{N}_{i,1} \cup \mathcal{N}_{i,2} \cup \cdots \cup \mathcal{N}_{i,m_i}$. It should be noted that the parameter m_i is predetermined and has nothing to do with $|\mathcal{N}_i|$.

The method of approximate average partitioning is adopted to ensure that the cardinality of each subset is approximately equal[1]. The cardinality $|\mathcal{N}_{i,g_i}|$ of the g_i-th subset can be expressed as:

$$|\mathcal{N}_{i,g_i}| = \lfloor |\mathcal{N}_i|/m_i \rfloor + \mathbb{I}(g_i \leq (|\mathcal{N}_i| \bmod m_i|)), \tag{8}$$

where $g_i = 1 : m_i$, and the indicator function $\mathbb{I}(\cdot)$ is defined as follows: when g_i is less than or equal to the remainder of $|\mathcal{N}_i|$ divided by m_i, $\mathbb{I}(\cdot)$ is 1, otherwise $\mathbb{I}(\cdot)$ is 0.

However, to ensure this performance lower bound, the gain values of all sensors need to be updated after each selection, and existing literature shows that this will bring huge computational complexity Mirzasoleiman et al. (2016). In fact, at the l-th selection at moment k, only the sensor $j^{l_{g_i^s}}_{g_i^s,select}$ in the g_i^s-th subset is selected. To reduce the amount of calculation, this section starts with the gain update method and explores the feasibility of only updating the gains of the remaining elements of the subset where the selected sensor is located.

Based on the inherent characteristics of the observable space of each sensor, this section investigates the mutual influence of gains between sensor subsets and proposes a set partitioning strategy to minimize the mutual influence of gains between subsets.

For the observable discrimination matrix $Q_{j,o}$ of neighbor sensor $j \in \mathcal{N}_i$ of sensor i, the indicator function for the ℓ-th row of the j-th sensor is defined as a binary indicator function:

$$I_{j,\ell} = \begin{cases} 1, & \exists m \in \{1, \ldots, n\},\ (Q_{j,o})_{\ell,m} \neq 0, \\ 0, & (Q_{j,o})_{\ell,:} = 0. \end{cases} \tag{9}$$

By calculating the indicator function for each row of $Q_{j,o}$, a column vector $[I_{j,\ell}]_{\ell=1:n} \in \mathbb{R}^n$ can be obtained. Then, the mutual influence is defined in Definition 2:

Definition 2. ***(Mutual Influence)*** *For any two sensors j_{g_i} and j_{q_i} in any neighbor sensor subsets $\mathcal{N}_{i,k,g_i}$ and $\mathcal{N}_{i,k,q_i}$ of sensor i, the mutual influence of gains between them is defined as the number of dimensions $[I_{j_{g_i},\ell}]_{\ell=1:n}$ and $[I_{j_{q_i},\ell}]_{\ell=1:n}$ that are not 0 simultaneously in all dimensions $\ell = 1 : n$, denoted as*

$$E(j_{g_i}, j_{q_i}) = [I_{j_{g_i},\ell}]_{\ell=1:n} \wedge [I_{j_{q_i},\ell}]_{\ell=1:n}. \tag{10}$$

And the problem of minimizing the mutual influence between subsets is given as shown below:

Problem 2. *During the selection of a suspicious sensor, assume that the sensor j_{g_i} from the g_i-th neighbor subset of sensor i, i.e., $j_{g_i} \in \mathcal{N}_{i,k,g_i}$, is selected. According to equation (9), the $Q_{j,o}$ of each sensor j can be transformed into an indicator function vector. Therefore, it is only necessary to ensure that mutual influence between the elements in other subsets q_i and the remaining elements of subset g_i is minimized, that is,*

$$\min_{q_i, j_{q_i}} \sum_{q_i=1, q_i \neq g_i}^{m_i} \sum_{j_{q_i} \in \mathcal{N}_{i,q_i}} E(j_{g_i}, j_{q_i}). \tag{11}$$

At this point, an optimal set partitioning algorithm based on the observable discrimination matrix can be proposed, which can be calculated offline.

The observable part of each sensor is extracted based on the observable discrimination matrix, so the mutual influence of gain only occurs between sensors with intersections in the observable space. Therefore, based on the

[1] At this point, the balance between the number of attacked sensors in each subset and the attack intensity can be obtained intuitively. And the results from literature Suo et al. (2024c) indicate that the D-ADS algorithm guarantees a performance lower bound for each subset consistent with that of the ADS algorithm. The proof process is omitted here. Please refer to the Lemma 2 in APPENDIX A and B.

optimal set partitioning strategy, after each suspicious sensor is selected, only the gains of the sensors in the subset need to be updated. However, the observable spaces of the sensors in the same subset may not be exactly the same. This means that after each sensor selection, the number of dimensions that need to be updated in the estimated error vector of each sensor in the subset will be different, resulting in an inaccurate allocation ratio vector $p_{p,k}^{(l_p)}$.

3.2. The Suboptimal set partitioning strategy based on Grassmann distance

Based on the previous analysis, this paper considers exploring a suboptimal partitioning strategy to strike a balance between the mutual influence between subsets and the correlation within subsets.

Inspired by the fact that Grassmann distance describes the angular differences in the directions of the vector spanning the subspace, the directional differences between the observable spaces of sensors in the subset are used to evaluate the correlation between sensors. First, the definition of Grassmann distance is introduced.

Definition 3. ***(Grassmann Distance)****Edelman, Arias and Smith (1998) For two subspaces U and V, the Grassmann distance $d_G(U, V)$ can be calculated by performing singular value decomposition on the bases of these two subspaces, i.e.,*

$$d_G(U, V) = \sqrt{\sum_{i=1}^{m} \theta_i^2}, \tag{12}$$

where m is the smaller dimension of U and V, and θ_i is the principal angle between U and V. Specifically, when the subspaces U and V are each spanned by one-dimensional vectors, $d_G(U, V) = \theta$.

Based on the indicator function column vector $[I_{j,\ell}]_{\ell=1:n}$ of all sensors $j \in \mathcal{N}_i$ in equation (9), the Grassmann distance between the observable spaces of each pair of sensors can be obtained. Then, the problem of assigning completely correlated sensors into the same subset can be described as Problem 3:

Problem 3. *For the g_i-th subset, the Grassmann distance between each pair of sensors $j_{g_i,1}, j_{g_i,2} \in \mathcal{N}_i$ can be obtained. Then, we only need to minimize the Grassmann distances between sensors within each subset $g_i = 1 : m_i$ to maximize the intra-subset correlation, i.e.,*

$$\min_{\theta_{j_{g_i,1},j_{g_i,2}}} \sum_{g_i=1:m_i} \|\boldsymbol{\theta_{g_i}}\|_2 = \|[\theta_{j_{g_i,1},j_{g_i,2}}]_{j_{g_i,1},j_{g_i,2} \in \mathcal{N}_{i,g_i}}\|_2. \tag{13}$$

For any two sensors j_1 and j_2 in the set $\mathcal{N}_i$, the cosine of the angle between their indicator function column vectors can be calculated using the vector dot product formula, i.e.,

$$\cos(\theta_{j_1,j_2}) = \frac{[I_{j_1,\ell}]_{\ell=1:n} \cdot [I_{j_2,\ell}]_{\ell=1:n}}{\|[I_{j_1,\ell}]_{\ell=1:n}\| \cdot \|[I_{j_2,\ell}]_{\ell=1:n}\|}. \tag{14}$$

The Grassmann distance between the observable spaces of sensors j_1 and j_2 can be determined using equation (15):

$$d_G([I_{j_1,\ell}]_{\ell=1:n}, [I_{j_2,\ell}]_{\ell=1:n}) = \arccos(\cos(\theta_{j_1,j_2})), \tag{15}$$

where the result is given in radians.

Remark 1. *It should be noted that equation (9) has already converted rows containing nonzero elements into binary values, either* 1 *or* 0*. As a result, the Grassmann distance calculated between the indicator function column vectors only has two possible outcomes: either the vectors are perfectly aligned ($\theta_{j_1,j_2} = 0$) or they are orthogonal ($\theta_{j_1,j_2} = \pi/2$). Ideally, for any g_i-th subset, the result of equation (13) should be zero.*

Based on the above analysis, the partitioning of the set $\mathcal{N}_i$ aims to find a compromise solution for two objectives: maximizing the intra-subset correlation and minimizing the mutual influence between subsets, and the correlation within the subset has a greater priority.

To reduce the computational cost incurred by calculating the Grassmann distance in step 13 of Algorithm 3.1, the improved algorithm is proposed in Algorithm 3.2. First, we present the following Lemma.

Algorithm 3.1 The Set Partitioning Strategy Based on Grassmann Distance

Input: The observable discrimination matrix $Q_{j,o}$ for all sensors $j \in \mathcal{N}_i$.
Output: The partitioning result of the sensor set $\mathcal{N}_i$.

Initialize $\mathcal{N}_{i,g_i}$, with $g_i = 1 : m_i$, and set the initial value of m_i to 1, which will increase dynamically.
for j in $\mathcal{N}_i$ **do**
    for $\ell = 1 : n$ **do**
        Calculate the indicator function $I_{j,\ell}$ for the ℓ-th row of $Q_{j,o}$ based on equation (9).
    end for
    Obtain the indicator function column vector $[I_{j,\ell}(k)]_{\ell=1:n} \in \mathbb{R}^n$.
end for
for $idx_1 = 1 : |\mathcal{N}_i|$ **do**
    found group = 0.
    for $g_i = 1 : m_i$ **do**
        $idx_2 = \mathcal{N}_{i,g_i}\{1\}$. % Take the first element from the set g_i.
        Calculate the cosine value of the angle between the indicator function column vectors of sensors j_{idx_1} and j_{idx_2}, which span a subspace, using equation (14).
        Calculate the Grassmann distance between the two subspaces using equation (15).
        if $d_G([I_{j_{idx_1},\ell}]_{\ell=1:n}, [I_{j_{idx_2},\ell}]_{\ell=1:n}) == 0$ **then**
            $\mathcal{N}_{i,g_i} = \mathcal{N}_{i,g_i} \cup \{j_{idx_2}\}$.
            found group = 1.
            break.
        end if
    end for
    if found group == 0 **then** % Create a new subset.
        $m_i = m_i + 1$.
        $\mathcal{N}_{i,m_i} = \mathcal{N}_{i,m_i} \cup \{j_{idx_2}\}$.
    end if
end for
return The g_i-th sensor subset $\mathcal{N}_{i,g_i}$, $g_i = 1 : m_i$.

Lemma 1. *A necessary but not sufficient condition for maximizing the intra-subset correlation is that all sensors within the subset have the same observable space dimension.*

PROOF. For any pair of two elements $j_{g_i,1}$ and $j_{g_i,2}$ within the g_i-th subset of sensor i, the intra-subset correlation of the g_i-th subset is defined as

$$\frac{\sum_{(j_{g_i,1},j_{g_i,2})\in\mathcal{N}_{i,g_i}\times\mathcal{N}_{i,g_i}} \mathbf{1}([I_{j_{g_i,1},\ell}]_{\ell=1:n} = [I_{j_{g_i,2},\ell}]_{\ell=1:n})}{|\mathcal{N}_{i,g_i}| \cdot |\mathcal{N}_{i,g_i}|}. \tag{16}$$

According to equation (16), when the indicator function vectors of two sensors are identical, they are fully correlated. In this case, their observable space dimensions must be the same. However, the converse does not necessarily hold. This complete the proof.

Inspired by Lemma 1, we first partition all sensors with the same dimension $Q_{j,o}$ into the same initial set. Then, we only need to apply Algorithm 3.1 separately in each set to partition the subsets. Theoretically, this strategy greatly reduces the computational cost required to calculate the Grassmann distance. The detailed steps are given in Algorithm 3.2.

Remark 2. ***(Computational Cost)*** *Given that the indicator function column vectors have the same dimension, the computational cost is proportional to the number of Grassmann distance calculations. In Algorithm 3.1, the number of Grassmann distance calculations is* $\binom{|\mathcal{N}_i|}{2}$. *Suppose the sensor set* $\mathcal{N}_i$ *can be divided into* m'_i *subsets based on dimension, then each subset contains approximately* $|\mathcal{N}_i|/m'_i$ *sensors. In the improved algorithm, the required number*

Algorithm 3.2 The improved sensor set partitioning strategy based on Grassmann distance

Input: The Cell array $Q_{total,o}$ consists of the observable matrices $Q_{j,o}$ of all sensors $j \in \mathcal{N}_i$.
Output: Set partitioning results of sensor set $\mathcal{N}_i$.

```
Initialize an empty Map object rankGroups.
for j = 1 : |N_i| do
    Obtain the observable matrix of sensor j by Q_{j,o} = Q_{total,o}{j}.
    Calculate the rank rank(Q_{j,o}) of each observable matrix Q_{j,o}.
    if isKey(rankGroups, rank(Q_{j,o})) then
        rankGroups(rank(Q_{j,o})) = [rankGroups(rank(Q_{j,o})) {Q_{j,o}}].
    else
        Create a key-value pair rankGroups(rank(Q_{j,o})) = Q_{j,o}.
    end if
end for
keys = rankGroups.keys.
for r = 1 : length(keys) do
    Output all observable matrices Q_{j,o} ∈ rankGroups(keys{r})) to Algorithm 3.1, and obtain the set partitioning
    result.
end for
return The g_i-th sensor subset N_{i,g_i}, g_i = 1 : m_i.
```

of Grassmann distance calculations is $m_i \cdot \binom{|\mathcal{N}_i|/m_i'}{2}$. *Comparing the two, the reduction in the number of Grassmann distance calculations is:*

$$\Delta C = \frac{|\mathcal{N}_i|^2(m_i' - 1) + |\mathcal{N}_i|}{2m_i'}. \tag{17}$$

Notably, when $m_i' > 1$, *this reduction is significant, implying that the improved algorithm effectively reduces the computational cost.*

Remark 3. *The proposed Algorithm 3.2 can ensure that the sensor observable space of each subset is consistent, but based on the D-ADS Algorithm, the theoretical performance of each subset is guaranteed only when the number of sensors in each subset is equal. Therefore, in the offline pre-setting stage, we need to ensure that the number of sensors with different observation spaces is equal, which is feasible.*

Theorem 1 will prove that based on the proposed set partitioning strategy, although the computational cost of updating the gain is reduced, the impact on the sensor selection performance is limited.

Theorem 1. *For the neighbour set* $\mathcal{N}_i$ *of sensor i, the set* $\mathcal{N}_i$ *is divided by Algorithm 3.2. At the* $l-1$*-th selection, suppose that an element* $j_s^{(l-1)}$ *is selected from one of the subset, and only the gains of the remaining sensors in the subset where the element is located are updated. Then, at the l-th selection, the distribution ratio vector of the sensor selection of any* g_i*-th subset* $\mathcal{N}_{i,k,g_i}$ *is accurate, or the error is tolerable.*

PROOF. According to the aforementioned analysis, there are 3 types of relationships between two sensors: Completely correlated, Partially correlated, Completely uncorrelated. Based on the set partitioning strategy shown in algorithm 3.2, the sensors within each subset are completely correlated, while these sensors are partially correlated or completely uncorrelated with the sensors in other subsets.

The distribution ratio vector error under 3 types of relationships are analyzed as follows:

For the case where the $l-1$-th selected sensor is completely uncorrelated with the l-th selected sensor, that is, there is no intersection in the observation spaces of the two sensors, the gain does not need to be updated at this time, and the distribution ratio vector error is 0.

For the case where the $l-1$-th selected sensor is completely correlated with the l-th selected sensor, that is, the observation spaces of the two sensors are exactly the same, the sensor gains are updated. Therefore, the distribution ratio vector error is also 0.

However, for the case where the $l-1$-th selected sensor is partially correlated with the l-th selected sensor, that is, the observation spaces of the two sensors intersect but are not exactly the same, so the gains of the two sensors have mutual influence. However, to reduce the computational cost, after the $l-1$th selection, the gain of the lth selected sensor is not updated, so there must be an error in the distribution ratio vector. The following proves that the distribution ratio vector error is bounded in this case.

For the $l-1$-th selected sensor $j_s^{(l-1)}$ and the l-th selected sensor $j_s^{(l)}$, the indicator function vectors are partially correlated. Considering the effect of diminishing marginal returns, the gain is most affected when the sensor is initially selected, and gradually decreases for subsequent selections. Therefore, the distribution ratio vector error is tolerable as long as the effect of the $l-1=1$-th selected sensor $j_s^{(1)}$ on the distribution ratio vector error of the $l=2$-th selected sensor $j_s^{(2)}$ is bounded.

Assuming that the diminishing marginal benefit of selecting sensor $j_s^{(1)}$ on the gain of $j_s^{(2)}$ is ignored, the gain $G^{(2)}_{k,j_s^{(2)}}$ of sensor $j_s^{(2)}$ is calculated as $G^{(2)}_{k,j_s^{(2)}} = f_k(\{j_s^{(2)}\})$. However, if the influence of selecting element $j_s^{(1)}$ on the gain of element $j_s^{(2)}$ is considered, the gain $G^{(2)}_{k,j_s^{(2)}}$ of sensor $j_s^{(2)}$ is calculated as $G^{(2)}_{k,j_s^{(2)}} = f_k(\mathcal{A}^{(1)}_{i,k} \cup \{j_s^{(2)}\}) - f_k(\mathcal{A}^{(1)}_{i,k})$. The absolute value of the gain error in the two cases is $\Delta_{j_s^{(1)},j_s^{(2)}}$, which actually indicates the change in the gain of $j_s^{(2)}$ caused by the influence of $j_s^{(1)}$ on the gain. Therefore, in the two cases, the distribution ratio vectors of the subset where the element $j^{(2)}$ belongs are respectively as shown below:

$$p' = \frac{[f_k(\{j^{(2)}\}]_{j^{(2)}\in\mathcal{N}_{i,k,g_i}}}{\sum_{j^{(2)}\in\mathcal{N}_{i,k,g_i}} f_k(\{j^{(2)}\})}, \tag{18}$$

$$p'' = \frac{[f_k(\{j^{(2)}\}) + \Delta_{j_s^{(1)},j^{(2)}}]_{j^{(2)}\in\mathcal{N}_{i,k,g_i}}}{\sum_{j^{(2)}\in\mathcal{N}_{i,k,g_i}} (f_k(\{j^{(2)}\}) + \Delta_{j_s^{(1)},j^{(2)}})}. \tag{19}$$

Therefore, the distribution ratio error $|p'(j_s^{(2)}) - p''(j_s^{(2)})|$ of any element $j_s^{(2)}$ in the set $\mathcal{N}_{i,k,g_i}$ is

$$\begin{aligned} & |p'(j_s^{(2)}) - p''(j_s^{(2)})| \\ = & \frac{|f_k(\{j_s^{(2)}\} \cdot \sum_{j^{(2)}\in\mathcal{N}_{i,k,g_i}} \Delta_{j_s^{(1)},j^{(2)}} - \sum_{j^{(2)}\in\mathcal{N}_{i,k,g_i}} f_k(\{j^{(2)}\}) \cdot \Delta_{j_s^{(1)},j_s^{(2)}}|}{(\sum_{j^{(2)}\in\mathcal{N}_{i,k,g_i}} f_k(\{j^{(2)}\})) \cdot (\sum_{j^{(2)}\in\mathcal{N}_{i,k,g_i}} (f_k(\{j^{(2)}\}) + \Delta_{j_s^{(1)},j^{(2)}}))} \\ \leq & \frac{\max_{j^{(2)}} \Delta_{j_s^{(1)},j^{(2)}} \cdot |f_k(\{j_s^{(2)}\} \cdot |\mathcal{N}_{i,k,g_i}| - \sum_{j^{(2)}\in\mathcal{N}_{i,k,g_i}} f_k(\{j^{(2)}\})|}{(\sum_{j^{(2)}\in\mathcal{N}_{i,k,g_i}} f_k(\{j^{(2)}\})) \cdot (\sum_{j^{(2)}\in\mathcal{N}_{i,k,g_i}} (f_k(\{j^{(2)}\}) + \Delta_{j_s^{(1)},j^{(2)}}))}, \end{aligned} \tag{20}$$

where the inequality holds because of $\Delta_{js^{(1)},js^{(2)}} \leq \max_{j^{(2)}} \Delta_{j_s^{(1)},j^{(2)}} = \Delta_{j_s^{(1)},j^{(2)}_{max}}$.

First, consider the special case where there is *no attack*. At this time, the gain of each sensor is only affected by noise. Therefore, from the perspective of the entire time period, the expectation of the gain $f_k(\{j^{(2)}\})$ of each element is theoretically 0, that is, $|f_k(\{j_s^{(2)}\} \cdot |\mathcal{N}_{i,k,g_i}| - \sum_{j^{(2)}\in\mathcal{N}_{i,k,g_i}} f_k(\{j^{(2)}\})|$ is also close to 0, which means that the increase of element $j_s^{(1)}$ leads to a negligible change in the gain of element $j^{(2)}$.

Furthermore, consider the case where there *exists attack*. Assume that q_{i,g_i} sensors in the g_i-th subset are attacked, while the remaining $|\mathcal{N}_{i,k,g_i}| - q_{i,g_i}$ sensors are normal. Then, the equation (20) is divided into two parts: $|f_k(\{j_s^{(2)}\} \cdot |\mathcal{N}_{i,k,g_i}| - \sum_{j^{(2)}\in\mathcal{N}_{i,k,g_i}} f_k(\{j^{(2)}\})|$ and $\Delta_{j_s^{(1)},j^{(2)}_{max}} / \left((\sum_{j^{(2)}\in\mathcal{N}_{i,k,g_i}} f_k(\{j^{(2)}\})) \cdot (\sum_{j^{(2)}\in\mathcal{N}_{i,k,g_i}} (f_k(\{j^{(2)}\}) + \Delta_{j_s^{(1)},j^{(2)}}))\right)$.

For the former, define a $0-1$ binary parameter ρ, whose values 0 and 1 represent the states of sensor $j_s^{(2)}$ is under attack (denoted as $j_s^{(2),u}$) and without attack (denoted as $j_s^{(2),w}$), respectively. At this time, the following derivation is

obtained

$$
\begin{aligned}
& |f_k(\{j_s^{(2)}\} \cdot |\mathcal{N}_{i,k,g_i}| - \sum_{j^{(2)} \in \mathcal{N}_{i,k,g_i}} f_k(\{j^{(2)}\})| \\
= \; & |f_k(\{j_s^{(2)}\} \cdot |\mathcal{N}_{i,k,g_i}| - \sum_{j^{(2),w} \in \mathcal{N}_{i,k,g_i} \setminus I_{i,k,g_i}} f_k(\{j^{(2),w}\}) - \sum_{j^{(2),u} \in I_{i,k,g_i}} f_k(\{j^{(2),u}\})| \\
\leq \; & \rho \cdot \Big(|\mathcal{N}_{i,k,g_i}| - q_{i,g_i} \Big) \, | \min_{j^{(2),w} \in \mathcal{N}_{i,k,g_i} \setminus I_{i,k,g_i}} f_k(\{j^{(2),w}\}) - \max_{j^{(2),u} \in I_{i,k,g_i}} f_k(\{j^{(2),u}\})| \\
& +(1-\rho) \cdot q_{i,g_i} \cdot | \max_{j^{(2),u} \in I_{i,k,g_i}} f_k(\{j^{(2),u}\}) - \min_{j^{(2),w} \in \mathcal{N}_{i,k,g_i} \setminus I_{i,k,g_i}} f_k(\{j^{(2),w}\})| \\
= \; & \max\{|\mathcal{N}_{i,k,g_i}| - q_{i,g_i}, q_{i,g_i}\} |f_k(\{j_{max}^{(2),u}\}) - f_k(\{j_{min}^{(2),w}\})|,
\end{aligned} \tag{21}
$$

where I_{i,k,g_i} in the first equation represents the set of all attacked sensors in the set N_{i,k,g_i}, and the first inequality holds because the maximum error that the selected sensor may bring is the maximum gain in the attacked sensor set and the minimum gain in the normal sensor set. In the second equation, $j_{max}^{(2),u}$ and $j_{min}^{(2),w}$ are equal to $\max_{j^{(2),u} \in I_{i,k,g_i}} f_k(\{j^{(2),u}\})$ and $\min_{j^{(2),w} \in \mathcal{N}_{i,k,g_i} \setminus I_{i,k,g_i}} f_k(\{j^{(2),w}\})$, respectively.

In addition, the parameter $\mu_{ij}^{(u)}(k)$ ($\mu_{ij}^{(w)}(k)$) is defined as the estimation error when the communication link between sensor j and i is under attack (without attack), which only depends on the network effect and the measurement noise and process noise of sensors i and j. By taking the expectation of equation (21) and omitting the subscripts max and min, we can get:

$$
\begin{aligned}
& \mathbb{E}\left[\max\{|\mathcal{N}_{i,k,g_i}| - q_{i,g_i}, q_{i,g_i}\} \cdot |f_k(\{j^{(2),u}\}) - f_k(\{j^{(2),w}\})|\right] \\
\leq \; & \mathbb{E}\left[\max\{|\mathcal{N}_{i,k,g_i}| - q_{i,g_i}, q_{i,g_i}\} \cdot \frac{|f_k(\{j^{(2),u}\})^2 - f_k(\{j^{(2),w}\})^2|}{|f_k(\{j^{(2),u}\}) + f_k(\{j^{(2),w}\})|}\right] \\
= \; & \mathbb{E}\left[\max\{|\mathcal{N}_{i,k,g_i}| - q_{i,g_i}, q_{i,g_i}\} \cdot \frac{(z_{i,j^{(2),u}} + \mu_{i,j^{(2),u}}^{u})^2 - (\mu_{i,j^{(2),w}}^{w})^2}{|z_{i,j^{(2),u}} + \mu_{i,j^{(2),u}}^{u} + \mu_{i,j^{(2),w}}^{w}|}\right] \\
\leq \; & \mathbb{E}\left[\max\{|\mathcal{N}_{i,k,g_i}| - q_{i,g_i}, q_{i,g_i}\} \cdot \frac{(z_{i,j^{(2),u}})^2 + 2z_{i,2}\mu_i^u + (\mu_i^u)^2 - (\mu_i^w)^2}{|z_{i,j^{(2),u}} + \mu_{i,j^{(2),u}}^{u} + \mu_{i,j^{(2),w}}^{w}|}\right] \\
\leq \; & \max\left\{ \lfloor \frac{|\mathcal{N}_i| - q_i}{m_i} \rfloor + \mathbb{I}(g_i \leq (|\mathcal{N}_i| \; mod \; m_i|)), \frac{q_i}{m_i} \right\} \cdot \frac{(\sum_{l=1}^{q_i} \phi_{i,q_i}(k)/q_i + 2||\mu_i(k)||_\infty^2)}{\bar{\mu}_i(k)},
\end{aligned} \tag{22}
$$

where the first inequality is obtained by multiplying both the numerator and the denominator by $|f_k(\{j^{(2),u}\}) + f_k(\{j^{(2),w}\})|$. The first equality holds because the values of $f_k(\{j^{(2),u}\})$ and $f_k(\{j^{(2),w}\})$ are essentially related to the attack signal $z_{i,j^{(2),u}}$ and the estimation error $\mu_{i,j^{(2),u}}^{u}$ ($\mu_{i,j^{(2),w}}^{w}$). The third inequality holds because $z_{i,j^{(2),u}}(k)$ and $\mu_{i,j^{(2),u}}^{u}(k)$ are completely independent over the entire time period, and the expectation of the attack signal $z_{i,j^{(2),u}}^2$ on any sensor $j^{(2),u}$ is approximately $1/q_i$, which is the sum of the average malicious perturbation power of all attacks, expressed as $\mathbb{E}[z_{i,j^{(2),u}}(k)^2] = \sum_{l=1}^{q_i} \phi_{i,q_i}(k)/q_i$. In addition, the estimated error $\mu_{ij}(k)$ satisfies $||\mu_i(k)||_\infty = \max_{j \in \mathcal{N}_i} \left\{ ||\mu_{ij}(k)||_\infty \right\}$ and the estimation error $\mu_{ij}(k)$ satisfies $|z_{i,j^{(2),u}}(k)| \geq \left\|\mu_i(k)\right\|_\infty \geq |\sum_{j \in \mathcal{N}_i} \mu_{ij}(k)|/|\mathcal{N}_i| = \bar{\mu}_i$.

For the latter of equation (20), dividing both the numerator and denominator by $\Delta_{j_s^{(1)}, j_{max}^{(2)}}$, we get

$$
1/\left((\sum_{j^{(2)} \in \mathcal{N}_{i,k,g_i}} f_k(\{j^{(2)}\})) \cdot \left(\frac{\sum_{j^{(2)} \in \mathcal{N}_{i,k,g_i}} (f_k(\{j^{(2)}\}) + \Delta_{j_s^{(1)}, j^{(2)}})}{\Delta_{j_s^{(1)}, j_{max}^{(2)}}} \right) \right). \tag{23}
$$

Since $\sum_{j^{(2)} \in \mathcal{N}_{i,k,g_i}} (f_k(\{j^{(2)}\}) + \Delta_{j_s^{(1)}, j^{(2)}}) \gg f_k(\{j^{(2)}\}) + \Delta_{j_s^{(1)}, j^{(2)}} > \Delta_{j_s^{(1)}, j_{max}^{(2)}}$ always holds, equation (23) is an infinitesimal positive number.

Considering the two parts of equation (20), ideally, $|p'(j_s^{(2)}) - p''(j_s^{(2)})| \to 0$, because a bounded positive number multiplied by an infinitesimal number tends to 0. In practice, we only need to ensure $|p'(j_s^{(2)}) - p''(j_s^{(2)})| \leq \epsilon$, which is obviously achievable. This also means that based on the proposed set partitioning strategy, only the gains of the remaining sensors in the subset where the selected sensor is located need to be updated, instead of the gains of all the remaining sensors, which will significantly reduce the calculation of the gains. This complete the proof.

4. Simulation Results

In this section, simulation experiments using the vehicle target state estimation are presented to illustrate the effectiveness of the proposed algorithm. Consider the following moving vehicle model(Zhou, Yang, Zhang, Zheng, Xu and Tang, 2022),

$$\begin{bmatrix} p_x(k+1) \\ p_y(k+1) \\ v_x(k+1) \\ v_y(k+1) \end{bmatrix} = \begin{bmatrix} 1 & 0 & 1/50 & 0 \\ 0 & 1 & 0 & 1/50 \\ 0 & 0 & 1 & 0 \\ 0 & 0 & 0 & 1 \end{bmatrix} \begin{bmatrix} p_x(k) \\ p_y(k) \\ v_x(k) \\ v_y(k) \end{bmatrix} + \omega(k), \tag{24}$$

where $p_x(k)$, $p_y(k)$, $v_x(k)$, and $v_y(k)$ represent the position and velocity of the vehicle in the x and y directions at moment k, respectively. The initial state of the vehicle is $x(0) = \begin{bmatrix} 50 & 0 & 5 & 0 \end{bmatrix}^T$. In the subsequent simulations, the initial state estimates of all sensors, $\hat{x}_i(0)$, are set to $x(0)$.

This simulation considers 2 kinds of sensor network scenarios to validate the performance of the proposed algorithm:

1. Scenario 1: A single central sensor and 100 neighboring sensors in an ultra-large-scale network.
2. Scenario 2: A complex distributed network with 500 sensors.

Scenario 1: In this scenario, a central sensor (labeled 0) is considered, along with 100 neighboring sensors (labeled 1–100). Each sensor independently measures the state of the vehicle, with the measurement model given by:

$$y_i(k) = C_i x(k) + v_i(k). \tag{25}$$

where the measurement matrix for the central sensor is $C_0 = [1 \quad 0 \quad 0 \quad 0]$. The measurement matrices for the neighboring sensors differ based on their observable state space, and are given by the following four types:

$$\begin{aligned} C_1 &= [1 \quad 0 \quad 0 \quad 0], \quad C_2 = [0 \quad 1 \quad 0 \quad 0], \\ C_3 &= [0 \quad 0 \quad 1 \quad 0], \quad C_4 = [0 \quad 0 \quad 0 \quad 1]. \end{aligned} \tag{26}$$

The process noise ω and measurement noise v_i are set with parameters $Q = 0.5I$ and $R_i = 0.5I$, respectively. Additionally, both the process noise and the measurement noise are bounded, i.e., $||\omega(k)||_\infty \leq 0.05$ and $||v_i(k)||_\infty \leq 0.05$ at all times. The observability matrices for each sensor are given by:

$$\begin{aligned} Q_{1,o} &= \begin{bmatrix} 1 & 1 & 1 & 1 \\ 0 & 0 & 0 & 0 \\ 0 & 1 & 2 & 3 \\ 0 & 0 & 0 & 0 \end{bmatrix}, \quad Q_{2,o} = \begin{bmatrix} 0 & 0 & 0 & 0 \\ 1 & 1 & 1 & 1 \\ 0 & 0 & 0 & 0 \\ 0 & 1 & 2 & 3 \end{bmatrix}, \\ Q_{3,o} &= \begin{bmatrix} 0 & 0 & 0 & 0 \\ 0 & 0 & 0 & 0 \\ 1 & 1 & 1 & 1 \\ 0 & 0 & 0 & 0 \end{bmatrix}, \quad Q_{4,o} = \begin{bmatrix} 0 & 0 & 0 & 0 \\ 0 & 0 & 0 & 0 \\ 0 & 0 & 0 & 0 \\ 1 & 1 & 1 & 1 \end{bmatrix}. \end{aligned} \tag{27}$$

It can be seen that the observability dimensions for the different types of sensors are varied, with dimensions of 1 and 3, 2 and 4, 3, and 4, respectively. It is assumed that the measurement matrix of sensors 1–25 is C_1, the measurement matrix of sensors 26–50 is C_2, the measurement matrix of sensors 51–75 is C_3, and the measurement matrix of sensors 76–100 is C_4. Additionally, all neighboring sensors $j \in \mathcal{N}_0$ are capable of transmitting information to the central sensor, with the transmitted information being the state estimate $\hat{x}_{0,j}(k)$, which may be compromised by FDIAs. Based

Table 1
Inter-subset Interaction and intra-subset Correlation under different Partitioning Strategy

Strategy	Set	Subset 1	Subset 2	Subset 3	Subset 4	Intra-subset Correlation	
Strategy 1	Subset 1		0			Subset 1	0.5
	Subset 2	0				Subset 2	0.5
Strategy 2	Subset 1		0	625	0	Subset 1	1
	Subset 2	0		0	625	Subset 2	1
	Subset 3	625	0		0	Subset 3	1
	Subset 4	0	625	0		Subset 4	1
Strategy 3	Subset 1		158	160	167	Subset 1	0.293
	Subset 2	158		140	156	Subset 2	0.28
	Subset 3	160	140		170	Subset 3	0.306
	Subset 4	167	156	170		Subset 4	0.2608

on the set partitioning strategy in Algorithm 3.2, the 100 sensors are divided into four subsets: sensors 1–25 form subset 1, sensors 26–50 form subset 2, sensors 51–75 form subset 3, and sensors 76–100 form subset 4.

At any moment, the attacker randomly selects 40 sensors to attack from 100 neighboring sensors. For any consecutive moments, the sets of attacked sensors $\mathcal{A}_{0,k}$ and $\mathcal{A}_{0,k-1}$ in the neighborhood of sensor 0 satisfy $\Delta_{0,k} = (\mathcal{A}_{0,k} \backslash \mathcal{A}_{0,k-1}) \cup (\mathcal{A}_{0,k-1} \backslash \mathcal{A}_{0,k}) \geq 0$.

In this simulation, only the velocity estimate $\hat{x}_{0,j}(k)$ in the sensor's estimated results is tampered with by the attacker, while the position estimate remains unaffected. The attack signals are classified into two types: one type corresponds to a unstealthy attack, which exhibits large magnitudes most of the time; the other type corresponds to a stealthy attack, whose magnitude is close to the estimation noise most of the time. To better simulate different attack scenarios, the attack signals are designed based on the magnitude of the estimation noise, ensuring that stealthy and unstealthy attacks do not appear in the same simulation experiment. This setup meets the prerequisites of Lemma 2 shown in the APPENDIX A.

According to Kalman decomposition (Suo, Chai, Chai, Farhan, Xia and Liu, 2024b), by first deinfluence and then reconstruction, the estimated error $\Delta\hat{x}_j^{re}$ of each sensor i and its neighbor sensor $j \in \mathcal{N}_i$, which only contains the observable part, can be obtained. The augmented error matrix $\Lambda_{i,k}$ in equation (6) is obtained by summarizing the $\Delta\hat{x}_j^{re}$ of all neighbors j. It should be noted that the number of non-zero rows of $\Delta\hat{x}_j^{re}$ and $Q_{j,o}$ is the same.

Next, we compare the distribution of inter-subset gain mutual influence and intra-subset correlation under different partitioning strategies. Three partitioning strategies are considered: the partitioning strategy based on minimizing inter-subset gain mutual influence (Partitioning Strategy 1), the suboptimal sensor partitioning strategy based on the Grassmann distance (Partitioning Strategy 2), and the random division of 100 sensors into 4 groups (Partitioning Strategy 3). For Partitioning Strategy 1, the observable spaces of C_1 (C_2) and C_3 (C_4) overlap. Consequently, the partitioning result is that subset 1 includes all sensors with measurement matrices C_1 and C_3, while subset 2 includes all sensors with measurement matrices C_2 and C_4. As shown in TABLE 1, the inter-subset benefit influence is 0, while the intra-subset correlation is 0.5, indicating that this strategy minimizes the inter-subset gain mutual influence. For Partitioning Strategy 2, sensors are fully correlated only when their measurement matrices are identical. Thus, the partitioning result consists of 4 subsets, each containing one type of sensor. As shown in TABLE 1, the inter-subset gain mutual influence is 625, while the intra-subset correlation is 1, indicating that this strategy maximizes intra-subset correlation. For Partitioning Strategy 3, by averaging the results of 100 completely independent partitioning instances, we obtain the results shown in TABLE 1, where neither the inter-subset gain mutual influence nor the intra-subset correlation is optimal. Therefore, the proposed suboptimal partitioning strategy achieves the goal of minimizing inter-subset gain mutual influence while maximizing intra-subset correlation.

Again, to verify the conclusion of Theorem 1, this simulation considers a special scenario where, at the first selection of each moment, the D-ADS algorithm always selects an attacked sensor from the subset 4.

According to Theorem 1, the gain interactions only exist between C_2 and C_4, that is, under these two gain update strategies, the error in the distribution ratio vector only appears in subset 2. The error curves are shown in Figure 1. To make the error curves smoother and more intuitive, the evaluation metric used is windowed RMSEs (W-RMSEs), with a window size of 10 moments. It can be observed that the distribution ratio vector error in subset 2 is bounded, with an average value of only $2.2871e-04$ over the entire time period, while the errors in subsets 1, 3, and 4 remain zero throughout, which is consistent with the conclusion of Theorem 1.

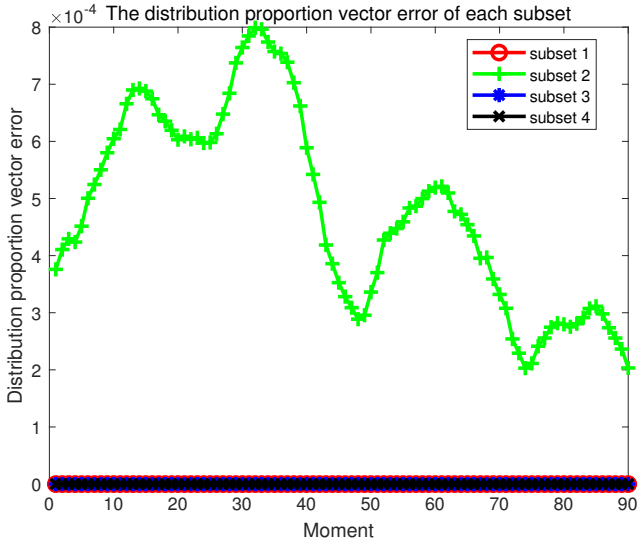

Figure 1: Distribution ratio vector error of the proposed partitioning strategy under different gain update methods

Scenario 2: Next, this simulation verifies that the proposed algorithm can ensure the secure state estimation of the system. Consider a complex distributed network scenario in which 500 sensors (labeled $1-500$) are randomly deployed in a 200m ×200m area. Each sensor has the capability to communicate with sensors within a 30m radius, forming an undirected graph. Similar to Scenario 1, each sensor can independently measure the state of the vehicles, and the measurement matrix is classified into the 4 types given in equation (26). First, measurement matrices are randomly assigned to the 500 sensors, and the number of each type of sensor in the neighbor set of each sensor is recorded. The statistical results indicate that, for almost all sensors, their neighbor sets fail to satisfy the requirement stated in Remark 3, which mandates an equal number of sensors observing different state spaces. In this case, based on the set partitioning result, the communication direction between sensors is dynamically adjusted to control the distribution of neighbor sensors of each sensor. Ultimately, the entire network is transformed into a directed graph, ensuring that the neighbor set of each sensor satisfies Remark 3. Therefore, based on the proposed Algorithm 3.1 or Algorithm 3.2, the neighbor set of each sensor can be divided into 4 subsets.

At each moment $k = 1 : 100$, the attacker randomly selects no more than half of the target sensors from the set of neighboring sensors of each sensor and launches stealthy attacks on their communication links. Therefore, the estimation results transmitted between sensors may be affected by FDIAs. Based on the D-ADS Algorithm, each sensor can preliminarily exclude a suspicious sensor set before fusing the information from neighboring sensors. This simulation compares the security of the system under different cases, including the case without attack detection, the case using the proposed D-ADS algorithm, and the case without any attack. For the no-attack scenario, the mean of the estimation errors of all sensors at each moment is used to calculate the RMSE. In contrast, for the case where attacks exist, considering that the security of the system can be intuitively described by the maximum estimation error, this simulation calculates the RMSE using the maximum estimation error at each moment. Figure 2 presents the RMSE curves under these cases, where there are three curves in total: the no-attack case (red), the proposed D-ADS algorithm detection (blue), and the case without attack detection (green). It can be seen that the blue curve is significantly lower than the green curve, indicating that the proposed algorithm ensures system security. However, there is still a certain gap

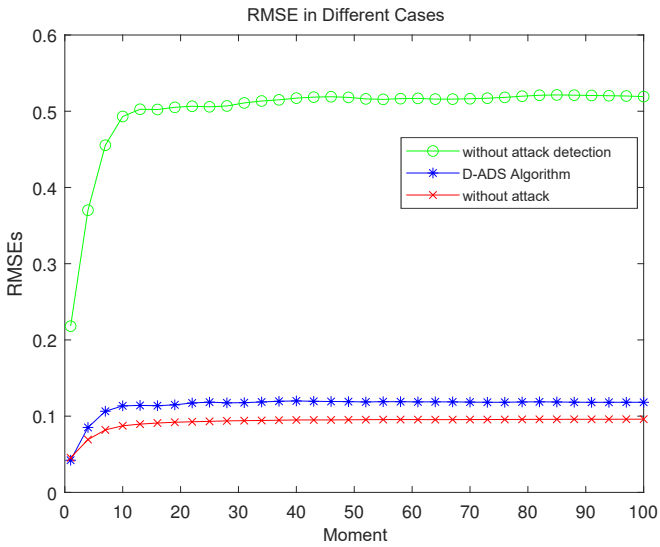

Figure 2: RMSE Curves under Different Cases

between the blue and red curves, as stealthy attacks are challenging to detect accurately. This observation is consistent with the simulation results in Scenario 1.

5. Conclusions

This paper investigates the performance of distributed attack detection scheduling algorithms in large-scale IoT networks. By analyzing the gain mutual influence between sensor subsets, an set partitioning strategy based on Grassmann distance is proposed, effectively reducing inter-subset mutual influence while enhancing intra-subset correlation. Theoretical analysis and simulation results demonstrate that the proposed strategy not only significantly narrows the performance gap between the D-ADS and ADS algorithm but also reduces computational cost. Future research can explore more advanced feature extraction methods to better capture complex information within the network, thereby further improving the efficiency and accuracy of attack detection.

6. APPENDIX A: The balance of the attack strategy

According to Assumption 1, at each moment, the attacker randomly selects q_i sensors from the neighbor set $\mathcal{N}_i$ of sensor i to launch the FDIAs, and the attack strategy satisfies the dynamic attack strategy in Definition 1. Lemma 2 will analyze the balance between the number of attacked sensors and the attack intensity in each subset.

Lemma 2. *Based on the Assumption 1, during the entire time period, the expectation of the number of attacked sensors in the g_i-th subset $\mathcal{N}_{i,g_i}$ of sensor i is $\mathbb{E}[q_{i,g_i}] = \lfloor q_i/m_i \rfloor$. In addition, the intensity of the attack on each subset is also balanced. Both are independent of the sensor set partitioning strategy, provided that the attacker selects the sensor to be attacked completely randomly at each moment, and the cardinality of each subset is approximately average.*

PROOF. Assume that the set of neighboring sensors of sensor i has been approximately divided into m_i subsets, the expected number of attacked sensors and the balance of attack intensity in each subset will be analyzed.

First, let's analyze the expected number of attacked sensors in each subset. Since the set of attacked sensors changes randomly at each moment, we estimate the mathematical expectation of the total number of attacked sensors over the entire period using the Monte Carlo method. The probability of a sensor being selected as an attack target is $q_i/|\mathcal{N}_i|$. Therefore, the expected number of attacked sensors in each subset is given by:

$$\mathbb{E}[q_{i,g_i}] = |\mathcal{N}_{i,g_i}| \times \left(\frac{q_i}{|\mathcal{N}_i|}\right) \approx \frac{|\mathcal{N}_i|}{m_i} \times \frac{q_i}{|\mathcal{N}_i|} = \left\lfloor \frac{q_i}{m_i} \right\rfloor.$$

Next, we consider the balance of attack intensity. In the literature Suo et al. (2024b), the average malicious disturbance power of the attack signal $z_{ij}(k)$ is defined as the average of the sum of the squared values of the attack signal $z_{ij}(k)$ on the communication link between sensor j and sensor i over the entire time period. However, since the attacked communication links vary dynamically at each moment, and the same link may experience different attacks at different moment, the definition in Suo et al. (2024b) is not applicable in this paper.

Therefore, this paper redefines the average malicious disturbance power from the attacker's perspective, rather than from the specific communication link's perspective. For the l-th attacker surrounding sensor i, where $l = 1 : q_i$, the average malicious disturbance power $\phi_{i,l}$ of the injected attack signal $z_{i,l}$ is defined as

$$\phi_{i,l} = \lim_{T\to\infty} \frac{1}{T} \sum_{k=1}^{T} \left(z_{i,l}(k)\right)^2 . \tag{28}$$

Based on the previous analysis, if the attacked sensors are completely random at each moment, the expected number of attacked sensors in each subset is $\lfloor q_i/m_i \rfloor$. Based on Assumption 1, the ratio of the average malicious disturbance power of each subset to the total malicious disturbance power of all attacks is $\lfloor q_i/m_i \rfloor / q_i = 1/m_i$. This indicates that the attack intensity in each subset is balanced. This completes the proof.

Then, a basic numerical simulation is utilized to verify that the attacker satisfies Lemma 2. Based on the set partitioning strategy in Algorithm 3.2, the 100 sensors are divided into four subsets: sensors 1–25 form subset 1, sensors 26–50 form subset 2, sensors 51–75 form subset 3, and sensors 76–100 form subset 4. Without considering specific attack types, at each time step, the attacker randomly selects 40 sensors for attack. The number of attacked sensors in each subset is shown in Figure 3. During the entire time period, the average number of sensors attacked in each subset was 9.83, 9.97, 10.04, and 10.16, respectively, which is close to the ideal average of 10.

Building on this, when specific attack types are considered, the attack intensity distribution for each subset is shown in Figure 4. The vertical axis represents the ratio of the attack intensity in each subset to the total attack signal intensity, which is ideally 0.25. It can be seen from Figure 4 that, the intensity ratios fluctuate around 0.25. Specifically, in Figure 4(a), the mean attack intensity ratios for each subset are 0.2497, 0.2500, 0.2504, and 0.2499, while in Figure 4(b), the mean ratios are 0.2507, 0.2490, 0.2499, and 0.2504.

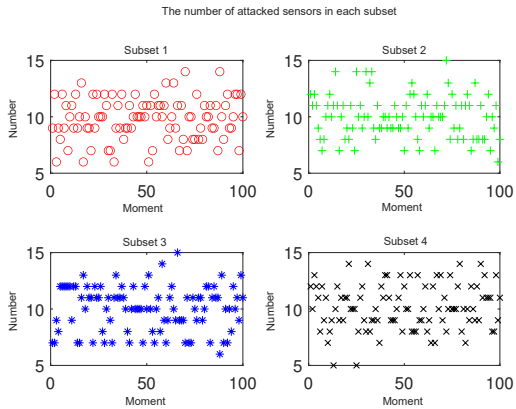

Figure 3: The number of attacked sensors in each subset

7. APPENDIX B: Distributed Attack Detection Scheduling Algorithm

The ADS algorithm in literature Suo et al. (2024c) can be extended to the D-ADS algorithm, as shown in Algorithm 3.3. The main difference between the D-ADS and ADS algorithms lies in the sensor selection method, specifically whether it uses centralized selection or distributed two-stage sensor selection. For the l-th selection at time step k, a suspicious sensor is first chosen from each subset (Stage 1 of sensor selection) and added to the set $S_k^{(l)}$. Then,

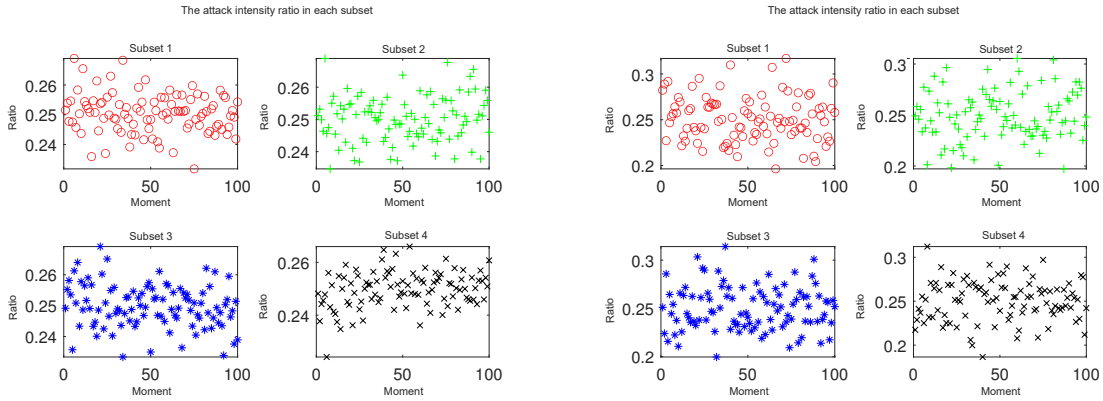

(a) Unstealthy attack

(b) Stealthy attack

Figure 4: Attack intensity ratio under unstealthy and stealthy attacks

Table 2
Summary of Variables in Algorithm 3.3

Parameter	Description
$\omega_{g_i,k}^{(l_{g_i})}$	The weight vector to be updated at the l_{g_i}-th selection for the g_i-th subset at moment k
$\mathcal{A}_{i,k,g_i^s}^{l_{g_i^s}}$	The set of suspicious sensors after the $l_{g_i^s}$-th selection for the g_i^s-th subset at moment k
$p_{g_i,k}^{(l_{g_i})}$	The distribution proportion vector at the l_{g_i}-th selection for the g_i^s-th subset at moment k
$\mathcal{S}_k^{(l)}$	The set of g_i sensors selected from all subsets at the l-th selection at moment k
$j_{g_i^s,select}^{l_{g_i^s}}$	The sensor selected in the $l_{g_i^s}$-th selection for the g_i^s-th subset
g_i^s	The subset to which the sensor $j_{g_i^s,select}^{l_{g_i^s}}$ selected from $\mathcal{S}_k^{(l)}$ belongs

a sensor is randomly selected from $\mathcal{S}_k^{(l)}$ as the result of the l-th selection (Stage 2 of sensor selection). The algorithm terminates when $|\mathcal{A}_{i,k}^{(l)}| = q_i$.

It should be noted that in steps 4-7, the gains of all remaining sensors $j \in \mathcal{N}_i \backslash \mathcal{A}_{i,k}^{(l-1)}$ are updated. However, with the improved partitioning strategy, only the gains of one subset of sensors need to be updated here. The meanings of the parameters in Algorithm 3.3 are summarized in TABLE 2[2].

Next, the performance relationship between the D-ADS algorithm in this paper and the ADS algorithm in literature Suo et al. (2024c) is analyzed. Both algorithms aim to select the set of suspicious sensors that have the greatest impact on the objective function (6). Therefore, ideally, their performance is consistent, meaning that $\mathcal{A}_{i,k} = \cup_{g_i=1}^{m_i} \mathcal{A}_{i,k,g_i}$.

Lemma 3. *For $g_i \in \{1, ..., m_i\}$, $l \in \{0, 1, ..., q_i\}$, define δ_{l,g_i} as $\delta_{l,g_i} = \sum_{k=1}^{T} (\frac{1}{m_i} f_k(\mathcal{A}_{i,k}^*) - f_k(\mathcal{A}_{i,k,g_i}^{(l_{g_i})}))$, where $\mathcal{A}_{i,k,g_i}^{(l_{g_i})}$ represents the set of suspicious sensors after the l_{g_i}-th selection of the g_i-th subset at moment k. Then, the relationship in literature Suo et al. (2024c) can be transformed as $\sum_{g_i=1}^{m_i} \delta_{l+1,g_i} - (1-\frac{1}{q_i})^{l+1} \sum_{g_i=1}^{m_i} \delta_{0,g_i} \leq \frac{m_i}{q_i} \sum_{j=1}^{l+1} (1-\frac{1}{q_i})^{l+1-j} B_i^{(j)}$. The parameter $B_i^{(l)}$ is described in detail in the proof. At this time, the Lemma 3.2 in literature Suo et al. (2024c) is extended to the distributed case.*

[2]Other variable symbols that are not explained here are the same as literature Suo et al. (2024c)

Algorithm 3.3 Distributed Attack Detection Scheduling Algorithm

Input: Neighbor set $\mathcal{N}_i$ of sensor i, maximum number of attacked neighboring sensors q_i, historical information values W_{kj}, $j \in \mathcal{N}_i$.

Output: Suspicious sensor set $\mathcal{A}_{i,k}$ at time k and $\mathcal{A}_{i,k,g_i} = \mathcal{A}^{(l)}_{i,k,g_i}$, where $g_i = 1 : m_i$, $k = 1, 2, ..., T$.

Initialize weight vector $\omega^{(l)}_k = [\omega^{(l)}_{kj}]_{j\in\mathcal{N}_i}$, where each element $\omega_{kj} = 1$, and set $\mathcal{A}^{(0)}_{i,k,g_i} = \emptyset$ for $p = 1 : m_i$, $k = 1 : T$, $l = l_{g_i} = 1$.
while $l < q_i$ **do**
    Set $\mathcal{S}^{(l)}_k = \mathcal{A}^{(l)}_{i,k} = \emptyset$.
    for all $j \in \mathcal{N}_i \backslash \mathcal{A}^{(l-1)}_{i,k}$ **do**
        % With optimized grouping strategies, only a subset of sensors' gains needs to be updated here.
        Compute $G^{(l)}_{kj} = f_k(\mathcal{A}^{(l-1)}_{i,k}) - f_k(\mathcal{A}^{(l-1)}_{i,k} \cup \{j\})$.
        Update $w^{(l)}_k$ as $w^{(l)}_{kj} = w^{(l-1)}_{k,j} e^{-G^{(l)}_{kj}}$.
    end for
    for $g_i = 1 : m_i$ **do**
        Set $w^{(l_{g_i})}_{g_i,k} = \left[w_{kj}\right]_{j\in\mathcal{N}_{i,g_i}\backslash\mathcal{A}^{(l_{g_i}-1)}_{i,k,g_i}}$.
        Compute $p^{(l_{g_i})}_{g_i,k} = w^{(l_{g_i})}_{g_i,k} / \|w^{(l_{g_i})}_{g_i,k}\|_1$.
        Select an element $j^{(l_{g_i})}_{g_i,select}$ based on the distribution vector $p^{(l_{g_i})}_{g_i,k}$. % Stage 1 sensor selection.
        Obtain $\mathcal{S}^{(l)}_k = \mathcal{S}^{(l)}_k \cup \{j^{(l_{g_i})}_{g_i,select}\}$.
    end for
    Randomly select an element $j^{(l_{g^s_i})}_{g^s_i,select}$ from $\mathcal{S}^{(l)}_k$. % Stage 2 sensor selection.
    Obtain $\mathcal{A}^{(l)}_{i,k} = \mathcal{A}^{(l-1)}_{i,k} \cup \{j^{(l_{g^s_i})}_{g^s_i,select}\}$.
    Obtain $\mathcal{A}^{(l_{g^s_i})}_{i,k,g^s_i} = \mathcal{A}^{(l_{g^s_i}-1)}_{i,k,g^s_i} \cup \{j^{(l_{g^s_i})}_{g^s_i,select}\}$.
    Update $l = l + 1$.
    Update $l_{g^s_i} = l_{g^s_i} + 1$.
end while
return $\mathcal{A}_{i,k}$ and $\mathcal{A}_{i,k,g_i} = \mathcal{A}^{(l)}_{i,k,g_i}$, where $g_i = 1 : m_i$.

PROOF. For the D-ADS algorithm, by summing δ_{l,g_i} over all m_i subsets and taking the average, we obtain

$$
\begin{aligned}
& \frac{1}{m_i}\sum_{g_i=1}^{m_i}\delta_{l,g_i} \\
\leq\ & \frac{1}{m_i}\sum_{k=1}^{T}(\sum_{g_i=1}^{m_i}(f_k(\mathcal{A}^*_{i,k,g_i}) - f_k(\mathcal{A}^{(l_{g_i})}_{i,k,g_i}))) \\
\leq\ & \frac{1}{m_i}\sum_{k=1}^{T}(\sum_{g_i=1}^{m_i}\sum_{j\in\mathcal{N}_{i,k,g_i}\backslash\mathcal{A}^*_{i,k,g_i}}(f_k(\mathcal{A}^{(l_{g_i})}_{i,k,g_i} \cup \{j^*_{kl}\}) - f_k(\mathcal{A}^{(l_{g_i})}_{i,k,g_i}))) \\
=\ & \frac{1}{m_i}\sum_{k=1}^{T}(\sum_{g_i=1}^{m_i}(-\sum_{j\in\mathcal{N}_{i,k,g_i}\backslash\mathcal{A}^*_{i,k,g_i}} G^{(l_{g_i}+1)}_{kj})),
\end{aligned}
\tag{29}
$$

!where the first inequality follows from $f_k(\mathcal{A}^*_{i,k}) \leq \sum_{g_i=1}^{m_i} f_k(\mathcal{A}^{(l_{g_i})}_{i,k,g_i})$, the second inequality follows from the submodularity of f_k, and the third equality follows from the definition of $G^{(l+1)}_{kj}$.

Based on Lemma 3 in literature Matsuoka, Ito and Ohsaka (2021), as well as the fact that $\delta_l \leq \sum_{g_i=1}^{m_i} \delta_{l,g_i}$ and $\delta_{l,g_i} \geq \delta_{l+1,g_i}$, we have

$$\frac{1-q_i}{m_i}\sum_{g_i=1}^{m_i}\delta_{l,g_i} \leq -\frac{q_i}{m_i}\left(\sum_{g_i=1}^{m_i}\delta_{l+1,g_i}\right) + B_i^{(l+1)},$$

where

$$B_i^{(l)} = \sum_{j=1}^{q_i}\sum_{k=1}^{T}\left(\frac{1}{m_i}\sum_{g_i=1}^{m_i} G^{(l_{g_i})}_{k,g_i} p^{(l_{g_i})}_{g_i,k} - G^{(l)}_{kj^*_{kl}}\right),$$

and $G^{(l_{g_i})}_{k,g_i} = [G^{(l)}_{kj}]_{j\in\mathcal{N}_{i,k,g_i}\setminus\mathcal{A}^{(l_{g_i}-1)}_{i,k,g_i}}$, with $G^{(l)}_{kj^*_{kl}}$ denoting the gain of the optimal sensor j^*_{kl} at time k in the l-th selection.

Thus, for all $l \in \{0, 1, ..., q_i\}$, the inequality

$$\sum_{g_i=1}^{m_i}\delta_{l+1,g_i} - \left(1-\frac{1}{q_i}\right)\sum_{g_i=1}^{m_i}\delta_{l,g_i} \leq \frac{m_i}{q_i}B_i^{(l+1)}$$

holds. After iterating, we obtain

$$\sum_{g_i=1}^{m_i}\delta_{l+1,g_i} - \left(1-\frac{1}{q_i}\right)^{l+1}\sum_{g_i=1}^{m_i}\delta_{0,g_i} \leq \frac{m_i}{q_i}\sum_{j=1}^{l+1}\left(1-\frac{1}{q_i}\right)^{l+1-j} B_i^{(j)}. \tag{30}$$

Thus, Lemma 1 in literature Suo et al. (2024c) has been extended to the distributed case. This completes the proof.

Theorem 2. *For the dynamic attack strategy in the Definition 1, the proposed D-ADS algorithm can ensure that the theoretical lower bound of the average optimization rate of suspicious sensor selection for any subset is $1-1/e$, and the error expectation is bounded.*

PROOF. To prove that the theoretical lower bound of the average optimization rate over the entire time period is $1-1/e$, we need to show that the expectation of the error

$$\mathbb{E}\left[\left(1-\frac{1}{e}\right)\sum_{k=1}^{T}\frac{1}{m_i}f_k\left(\mathcal{A}^*_{i,k}\right) - \sum_{k=1}^{T} f_k(\mathcal{A}_{i,k,g_i})\right] \tag{31}$$

is bounded, where $f_k\left(\mathcal{A}_{i,k,g_i}\right)$ represents the submodular function value for the selected suspicious sensor set in subset g_i at time k.

Essentially, the expectation of the error represents the expected difference between the objective function value of the selected suspicious sensor set and $1-1/e$ times the optimal suspicious sensor set's objective function value. Therefore, the larger the objective function value of a subset, the greater the upper bound of the error expectation. Consequently, the subset with the largest objective function value has the highest upper bound for error expectation, as shown in equation (32)

$$\begin{aligned} & (1-\frac{1}{e})\sum_{k=1}^{T}\frac{1}{m_i}f_k\left(\mathcal{A}^*_{i,k}\right) - \sum_{k=1}^{T}\max_{g_i} f_k(\mathcal{A}_{i,k,g_i}) \\ \leq\ & \frac{1}{m_i}\left[(1-\frac{1}{e})\sum_{k=1}^{T} f_k\left(\mathcal{A}^*_{i,k}\right) - \sum_{k=1}^{T} f_k(\mathcal{A}_{i,k})\right] \end{aligned} \tag{32}$$

$$\leq \quad \frac{1}{m_i}\left[(1-(1-\frac{1}{q_i})^{q_i})\sum_{k=1}^{T} f_k\left(\mathcal{A}^*_{i,k}\right)-\sum_{k=1}^{T} f_k\left(\mathcal{A}_{i,k}\right)\right],$$

where the first inequality follows from literature Mirzasoleiman et al. (2016), which states that $\max_{g_i} f_k(\mathcal{A}_{i,k,g_i}) \geq \frac{1}{m_i} f_k(\mathcal{A}_{i,k})$, and the second inequality follows from $(1-1/k)^k \leq 1/e$.

It is important to note that $\sum_{k=1}^{T} 1/m_i \cdot f_k\left(\mathcal{A}^*_{i,k}\right)$ does not imply that the objective function of each subset satisfies $\sum_{k=1}^{T} 1/m_i \cdot f_k\left(\mathcal{A}^*_{i,k}\right) = \sum_{k=1}^{T} f_k\left(\mathcal{A}^*_{i,k,g_i}\right)$. Instead, it follows from the assumption that the impact of attack signals on each subset is balanced over the entire time period.

Based on the Lemma 3 from literature Matsuoka et al. (2021) and the definition $\delta_l = \sum_{k=1}^{T}\left(f_k(\mathcal{A}^*_{i,k}) - f_k(\mathcal{A}^{(l)}_{i,k})\right)$ for $l = 1 : q_i$, we obtain that, $\sum_{k=1}^{T} f_k\left(\mathcal{A}^*_{i,k}\right) - \sum_{k=1}^{T} f_k\left(\mathcal{A}_{i,k}\right) + (1-(1-\frac{1}{q_i})^{q_i})\sum_{k=1}^{T}(f_k(\mathcal{A}^{(0)}_{i,k}) - f_k(\mathcal{A}^*_{i,k})) \leq \delta_{q_i} - (1-\frac{1}{q_i})^{q_i}\delta_0 \leq \sum_{g_i=1}^{m_i}\delta_{l,g_i} - (1-\frac{1}{q_i})^{q_i}\sum_{g_i=1}^{m_i}\delta_{0,g_i}$, where the inequality $\delta_{q_i} \leq \sum_{g_i=1}^{m_i}\delta_{l,g_i}$ follows from the diminishing marginal returns property of the submodular function, and the initial condition satisfies $\delta_0 = \sum_{g_i=1}^{m_i}\delta_{0,g_i}$. Combining equation (30) with the above relation, equation (32) can be rewritten as

$$\begin{aligned}
&(1-\frac{1}{e})\sum_{k=1}^{T}\frac{1}{m_i} f_k\left(\mathcal{A}^*_{i,k}\right) - \sum_{k=1}^{T}\max_{g_i} f_k(\mathcal{A}_{i,k,g_i}) \\
\leq \quad & \frac{m_i}{q_i}\sum_{j=1}^{q_i}(1-\frac{1}{q_i})^{q_i-j}\frac{B_i^{(j)}}{m_i}.
\end{aligned} \tag{33}$$

Thus, to prove that equation (32) is bounded, it suffices to show that $\mathbb{E}[B_i^{(l)}/m_i]$ is bounded

$$\begin{aligned}
&\mathbb{E}\left[\frac{B_i^{(l)}}{m_i}\right] \\
= \quad & \frac{1}{m_i}\sum_{j=1}^{q_i}\mathbb{E}\left[\sum_{k=1}^{T}\left(\frac{1}{m_i}\sum_{g_i=1}^{m_i} G_{k,g_i}^{\binom{l_{g_i}}{}} p_{g_i,k}^{\binom{l_{g_i}}{}} - G_{kj^*_{kl}}^{(l)}\right)\right] \\
\leq \quad & \frac{1}{m_i}\sum_{j=1}^{q_i}\mathbb{E}\left[\sum_{k=1}^{T}(G_k^{(l)} p_k^{(l)} - G_{kj^*_{kl}}^{(l)})\right] \\
\leq \quad & \frac{2q_i}{m_i}\sqrt{(2\Delta_T\log(|\mathcal{N}_i|T) + T(2\log(|\mathcal{N}_i|T) + \log(T)))},
\end{aligned} \tag{34}$$

where the first inequality follows from the arithmetic mean-geometric mean inequality, and the second follows from Theorem 2 in literature Suo et al. (2024c).

Thus, the expectation of the error in equation (31) is bounded

$$\begin{aligned}
&\mathbb{E}\left[\left(1-\frac{1}{e}\right)\sum_{k=1}^{T}\frac{1}{m_i} f_k\left(\mathcal{A}^*_{i,k}\right) - \sum_{k=1}^{T} f_k(\mathcal{A}_{i,k,g_i})\right] \\
\leq \quad & \tilde{\mathcal{O}}\left(\frac{q_i}{m_i}\sqrt{3T+2\Delta_T}\right),
\end{aligned} \tag{35}$$

where $\mathbb{E}[\cdot]$ represents expectation, and $\tilde{\mathcal{O}}$ hides logarithmic terms. This completes the proof.

CRediT authorship contribution statement

Yuhan Suo: Conceptualization, Methodology, Software, writing-original draft. **Runqi Chai:** Methodology, Writing - Review & Editing. **Kaiyuan Chen:** Writing - Review & Editing. **Senchun Chai:** Review, supervision. **Wannian Liang:** Writing - Review & Editing. **Yuanqing Xia:** Review.

Declaration of Interest

The authors declare that they have no known competing financial interests or personal relationships that could have appeared to influence the work reported in this paper. Generative AI and AI-assisted technologies are only applied to the writing process to improve the readability and language of the manuscript.

References

An, L., Yang, G.H., 2022. Fast state estimation under sensor attacks: A sensor categorization approach. Automatica 142, 110395.

Balta, E.C., Pease, M., Moyne, J., Barton, K., Tilbury, D.M., 2023. Digital twin-based cyber-attack detection framework for cyber-physical manufacturing systems. IEEE Transactions on Automation Science and Engineering 21, 1695–1712.

Ding, D., Han, Q.L., Ge, X., Wang, J., 2020. Secure state estimation and control of cyber-physical systems: A survey. IEEE Transactions on Systems, Man, and Cybernetics: Systems 51, 176–190.

Edelman, A., Arias, T.A., Smith, S.T., 1998. The geometry of algorithms with orthogonality constraints. SIAM journal on Matrix Analysis and Applications 20, 303–353.

Ge, X., Han, Q.L., Zhong, M., Zhang, X.M., 2019. Distributed krein space-based attack detection over sensor networks under deception attacks. Automatica 109, 108557.

Habibzadeh, H., Qin, Z., Soyata, T., Kantarci, B., 2017. Large-scale distributed dedicated-and non-dedicated smart city sensing systems. IEEE Sensors Journal 17, 7649–7658.

Hatami, M., Leinonen, M., Chen, Z., Pappas, N., Codreanu, M., 2022. On-demand aoi minimization in resource-constrained cache-enabled iot networks with energy harvesting sensors. IEEE Transactions on Communications 70, 7446–7463.

Heo, J., Hong, J., Cho, Y., 2009. Earq: Energy aware routing for real-time and reliable communication in wireless industrial sensor networks. IEEE Transactions on Industrial Informatics 5, 3–11.

Ju, Y., Wei, G., Li, W., 2023. Distributed fault estimation over sensor networks: A bit rate allocation scheme. Information Sciences 633, 597–612.

Li, T., Chen, B., Liu, S., Wang, Z., Zhang, W.A., Yu, L., 2023. Fast attack detection for cyber–physical systems using dynamic data encryption. IEEE Transactions on Cybernetics .

Li, Z., Chen, X., Chen, Y., Li, S., Wang, H., Lv, S., Sun, L., 2024. Detecting cyber-attacks against cyber-physical manufacturing system: A machining process invariant approach. IEEE Internet of Things Journal .

Lu, A.Y., Yang, G.H., 2023a. A polynomial-time algorithm for the secure state estimation problem under sparse sensor attacks via state decomposition technique. IEEE Transactions on Automatic Control 68, 7451–7465.

Lu, A.Y., Yang, G.H., 2023b. Secure state estimation under sparse sensor attacks via saturating adaptive technique. IEEE Transactions on Control of Network Systems 10, 1890–1898.

Matsuoka, T., Ito, S., Ohsaka, N., 2021. Tracking regret bounds for online submodular optimization, in: International Conference on Artificial Intelligence and Statistics, PMLR. pp. 3421–3429. doi:None.

Mirzasoleiman, B., Karbasi, A., Sarkar, R., Krause, A., 2016. Distributed submodular maximization. The Journal of Machine Learning Research 17, 8330–8373.

Mustafa, A., Mazouchi, M., Modares, H., 2022. Secure event-triggered distributed kalman filters for state estimation over wireless sensor networks. IEEE Transactions on Systems, Man, and Cybernetics: Systems 53, 1268–1283.

Pang, Z.H., Fan, L.Z., Dong, Z., Han, Q.L., Liu, G.P., 2021. False data injection attacks against partial sensor measurements of networked control systems. IEEE Transactions on Circuits and Systems II: Express Briefs 69, 149–153.

Shoukry, Y., Nuzzo, P., Puggelli, A., Sangiovanni-Vincentelli, A.L., Seshia, S.A., Tabuada, P., 2017. Secure state estimation for cyber-physical systems under sensor attacks: A satisfiability modulo theory approach. IEEE Transactions on Automatic Control 62, 4917–4932.

Smith, K.J., Dhillon, G., Carter, L., 2021. User values and the development of a cybersecurity public policy for the iot. International Journal of Information Management 56, 102123.

Suo, Y., Chai, R., Chai, S., Farhan, I., Zhao, X., Xia, Y., 2024a. Opinion dynamic under malicious agent influence in multi-agent systems: From the perspective of opinion evolution cost. arXiv preprint arXiv:2412.01524 .

Suo, Y., Chai, R., Chai, S., Farhan, I.M., Xia, Y., Liu, G.P., 2024b. Attack detection and secure state estimation of collectively observable cyber-physical systems under false data injection attacks. IEEE Transactions on Automatic Control 69, 2067–2074. doi:10.1109/TAC.2023.3316160.

Suo, Y., Chai, S., Chai, R., Pang, Z.H., Xia, Y., Liu, G.P., 2024c. Security defense of large-scale networks under false data injection attacks: An attack detection scheduling approach. IEEE Transactions on Information Forensics and Security 19, 1908–1921. doi:10.1109/TIFS.2023.3340098.

Tao, F., Zhang, Y., Cheng, Y., Ren, J., Wang, D., Qi, Q., Li, P., 2022. Digital twin and blockchain enhanced smart manufacturing service collaboration and management. Journal of Manufacturing Systems 62, 903–914.

Wang, Y., Lu, Z., Ma, J., Jin, Q., 2025. Locational false data injection attack detection in smart grid using recursive variational graph auto-encoder. IEEE Internet of Things Journal .

Wang, Z., Chen, H., Yang, X., Wan, J., Li, T., Luo, C., 2023. Fuzzy rough dimensionality reduction: a feature set partition-based approach. Information Sciences 644, 119266.

Wang, Z., Wang, N., Su, X., Ge, S., 2020. An empirical study on business analytics affordances enhancing the management of cloud computing data security. International Journal of Information Management 50, 387–394.

Wei, Z., Zhu, M., Zhang, N., Wang, L., Zou, Y., Meng, Z., Wu, H., Feng, Z., 2022. Uav-assisted data collection for internet of things: A survey. IEEE Internet of Things Journal 9, 15460–15483.

Xia, W., Zhou, M., 2025. Resilient distributed kalman filtering against malicious cyber attacks. IEEE Transactions on Aerospace and Electronic Systems .

Xie, H., Yan, Z., Yao, Z., Atiquzzaman, M., 2018. Data collection for security measurement in wireless sensor networks: A survey. IEEE Internet of Things Journal 6, 2205–2224.

Xin, L., He, G., Long, Z., 2025. Secure state estimation for multi-sensor cyber-physical systems using virtual sensor and deep reinforcement learning under multiple attacks on major sensor. IEEE Transactions on Network Science and Engineering .

Yang, T., Lv, C., 2021. Secure estimation and attack isolation for connected and automated driving in the presence of malicious vehicles. IEEE Transactions on Vehicular Technology 70, 8519–8528.

Zhang, J., Pan, L., Han, Q.L., Chen, C., Wen, S., Xiang, Y., 2021. Deep learning based attack detection for cyber-physical system cybersecurity: A survey. IEEE/CAA Journal of Automatica Sinica 9, 377–391.

Zhang, L., Xie, X., Xiao, K., Bai, W., Liu, K., Dong, P., 2022. Manomaly: Mutual adversarial networks for semi-supervised anomaly detection. Information Sciences 611, 65–80.

Zhao, Z., Xu, Y., Li, Y., Zhao, Y., Wang, B., Wen, G., 2023. Sparse actuator attack detection and identification: A data-driven approach. IEEE Transactions on Cybernetics 53, 4054–4064.

Zhou, J., Yang, W., Zhang, H., Zheng, W.X., Xu, Y., Tang, Y., 2022. Security analysis and defense strategy of distributed filtering under false data injection attacks. Automatica 138, 110151.